Polymer Chemistry

PAPER

View Article Online
View Journal | View Issue

Published on 26 April 2017. Downloaded by Synchrotron Radiation Library on 12/12/2017 06:20:03.

Check for updates

Cite this: *Polym. Chem.*, 2017, **8**, 3294

Dynamic supramolecular self-assembly: hydrogen bonding-induced contraction and extension of functional polymers†

Chih-Chia Cheng,* [a] Jui-Hsu Wang,[b] Wei-Tsung Chuang,[c] Zhi-Sheng Liao,[a] Jyun-Jie Huang,[a] Shan-You Huang,[a] Wen-Lu Fan[a] and Duu-Jong Lee[d,e,f]

Simple construction and manipulation of low-molecular-weight supramolecular polymers, based on incorporation of self-complementary multiple hydrogen bonding interactions, with the desired dynamic response characteristics to achieve high-efficiency supramolecular assembly and control the morphological properties of the polymers remain highly challenging. Herein, we developed a new difunctional telechelic supramolecular polymer (UrCy-PPG) containing self-complementary quadruple hydrogen-bonded ureido-cytosine (UrCy) moieties, which spontaneously self-assembles to form long-range-ordered lamellar structures in the bulk state. Scattering and rheological studies confirmed that the dynamic behavior of UrCy units induces structural phase transitions from quadruple to dual hydrogen-bonded arrays, leading to well-controlled, self-organized supramolecular nanostructure morphologies. The microstructural features could be easily tuned by altering environmental conditions, making the self-assembly processes highly efficient. Importantly, temperature/shear stress-dependent microstructural analyses indicated that UrCy-PPG has the capacity to manipulate the transition between contractile and fully extended lamellar structures. Given its novelty, simple synthesis, high reliability, and efficient self-assembly processes, this newly developed supramolecular polymer represents a new concept and pathway for controlled arrangement of self-assembled polymeric nanostructures.

Received 24th April 2017,
Accepted 25th April 2017

DOI: 10.1039/c7py00684e

rsc.li/polymers

Introduction

Synergistic self-assembly of supramolecular structures that function as building blocks to enable construction of functional polymers has attracted considerable interest among academic researchers and industry over the last decade.[1–5] Synthetic supramolecular structures, such as organic ligands and inorganic molecules, can be directly fabricated and manipulated by altering the intermolecular secondary interactions between atomic bonds, including π stacking, hydrogen bonding, electrostatic, van der Waals interactions, and metal–ligand bonds.[6–9] These interactions enable supramolecular polymers to spontaneously self-assemble into ordered structures to confer novel properties upon the host matrix, such as high-sensitivity environmental stimuli-responsive ability and unique physical characteristics.[10,11] Thus, the reversibility of the linkages between supramolecular polymer building blocks is an essential factor required to achieve critical coupling, especially in terms of bonding strength and the specificity of the supramolecular motifs.[6,12,13] Incorporation of nucleobase pairs into the polymeric building blocks used to create functional polymers is one of the most well-characterized supramolecular polymer self-assembly motifs. Strong (self-)complementary hydrogen bonds between adjacent nucleobases function as physical connection points that confer well-controlled self-assembly behavior to polymers, thus promoting the formation of long-period stacking ordered microstructures.[4,14,15] Therefore, polymeric microstructures constructed using nucleobase molecular recognition can enable the creation of various secondary structures to achieve the required supramolecular polymer properties.

The use of (self-)complementary multiple hydrogen-bonding (CMHB) interactions is an effective method of joining polymer chains *via* supramolecular assembly of multicompo-

[a]*Graduate Institute of Applied Science and Technology, National Taiwan University of Science and Technology, Taipei 10607, Taiwan.*
E-mail: cccheng@mail.ntust.edu.tw
[b]*Institute of Applied Chemistry, National Chiao Tung University, Hsin Chu 30050, Taiwan*
[c]*National Synchrotron Radiation Research Center, Hsinchu 30076, Taiwan*
[d]*Department of Chemical Engineering, National Taiwan University, Taipei 10617, Taiwan*
[e]*Department of Chemical Engineering, National Taiwan University of Science and Technology, Taipei 10607, Taiwan*
[f]*R&D Center for Membrane Technology, Chung Yuan Christian University, Chungli, Taoyuan 32043, Taiwan*

† Electronic supplementary information (ESI) available: All synthetic procedures and instrumentation used in this work. See DOI: 10.1039/c7py00684e

This journal is © The Royal Society of Chemistry 2017

Published on 26 April 2017. Downloaded by Synchrotron Radiation Library on 12/12/2017 06:20:03.

nent microstructures, eventually resulting in the formation of multifunctional polymers. The strength of the CMHB complexes can be tuned by altering the donor (D) and acceptor (A) sites to fabricate the desired polymeric architectures, without the need to covalently attach polymer chains. Polymers incorporating CMHB units have been confirmed to form transient non-covalent bonds that efficiently improve the mechanical and thermal properties of the polymers; the behavior of the polymers can be directly manipulated to alter dynamic properties and create a variety of stimuli-responsive supramolecular polymers.[16–20] Hailes and co-workers developed a new self-complementary quadruple hydrogen-bonded ureido-cytosine (UrCy) module with a stable DDAA array and high association constant ($K_a = 9 \times 10^6$ M^{-1} in deuterated benzene).[21] The UrCy groups are located at the ends of the polymers, and promote the formation of a highly ordered structure, thus resulting in unique physical properties.[22,23] Recently, we discovered that UrCy-functionalized polymers can be used to directly manipulate exfoliation of graphite nanoplatelets, enabling efficient exfoliation of natural graphite into micrometer-sized few-layered graphene sheets due to the specific interaction between graphene and UrCy moieties.[24] In addition, these polymers can also assemble into a long-range ordered lamellar nanostructure that effectively transports lithium within the well-ordered lamellar nanochannels; this material could potentially be applied in a wide range of energy devices.[25] Therefore, based on the research progress described above, we reasonably assumed that the presence of dynamic, reversible, self-complementary UrCy moieties in the polymer backbone would act as a polymeric conformational switch to profoundly affect the stimuli-responsive behavior of the resulting polymers and enable predictable tuning of the hierarchical microstructures under applied shear stress and at elevated temperature. Exploiting the reversible non-covalent bonding of UrCy moieties within polymer materials may provide significant benefits in the manipulation of polymeric self-assembly processes and confer improved microstructural predictability and controllability.

Recent studies performed in our laboratory demonstrated that supramolecular polymers prepared from a low molecular weight difunctional oligomer can efficiently self-assemble into nanosized micelles in an aqueous environment and possess a number of unique characteristics, including excellent thermo-responsive and self-assembly properties, as well as high drug-loading and well-controlled release capability due to the presence of the CMHB interactions.[26,27] These carriers have considerable potential to enhance the delivery of chemotherapeutic drugs directly to tumors while reducing overall toxicity.[27] Based on the research discussed above, this study extended our previous work to obtain a well-designed and efficiently produced UrCy-based supramolecular polymer *via* simple synthesis of oligomeric polypropylene glycol (PPG) end-capped with UrCy groups (UrCy-PPG). We demonstrate that introducing CMHB interactions *via* UrCy moieties confers this new material with the distinctive ability to spontaneously self-assemble into higher-level lamellar microstructures and behave as a polymer-like material in the bulk state. Shear stress and temperature-driven microstructural transitions were clearly noted in the bulk state for UrCy-PPG, which provides a dynamic, reversible self-organizing capability to manipulate the transition between contractile and fully extended lamellar microstructures (Scheme 1). To the best of our knowledge, the use of low-molecular-weight supramolecular polymers based on CMHB interactions with the aim of generating precisely controlled microstructures and achieving stable microstructural transitions has not yet been thoroughly explored. This study indicates that UrCy-based supramolecular polymers provide a simple, efficient pathway towards the development of new structural phase-transition polymers based on dynamic CMHB interactions.

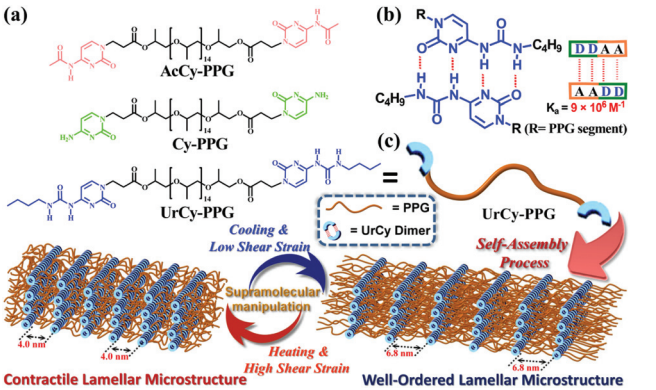

Scheme 1 (a) Chemical structures of oligomeric AcCy-PPG, Cy-PPG and UrCy-PPG. (b) Structural dimerization of UrCy *via* self-complementary quadruple hydrogen bonding. (c) Graphical representation of the self-assembly process of UrCy-PPG in the bulk state for the transition between the contractile and fully extended lamellar microstructures.

Results and discussion

A novel self-complementary UrCy-functionalized UrCy-PPG was successfully fabricated by a simple three-step synthesis procedure, as shown in Scheme S1 (see the ESI† for further details). First, we synthesized low-molecular-weight acetylcytosine (AcCy)-terminated PPG (AcCy-PPG) by a Michael addition reaction of PPG diacrylate (average molecular weight ~800, *ca.* 14 repeat units) with AcCy,[26] and then subsequently removed the acetyl protecting groups to obtain cytosine-terminated PPG (Cy-PPG). Finally, Cy-PPG was functionalized *via* an isocyanate-mediated reaction with *n*-butyl isocyanate to produce high yields (>90%) of UrCy-PPG, the chemical structure of which is illustrated in Scheme 1. With respect to their macroscopic states under ambient conditions, UrCy-PPG was a crystalline white powder, whereas AcCy-PPG and Cy-PPG were viscous liquids. This implies that the ability of UrCy-PPG to form a solid can be attributed to the intermolecular CMHB interactions between UrCy moieties that induce efficient packing of polymeric chains, and uniquely and drastically impact the macroscale structure of the supramolecular material. This

Published on 26 April 2017. Downloaded by Synchrotron Radiation Library on 12/12/2017 06:20:03.

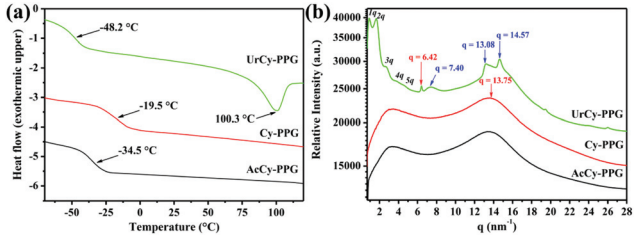

Fig. 1 (a) DSC curves and (b) WAXS data for AcCy-PPG, Cy-PPG and UrCy-PPG.

interesting observation motivated us to study the phase behavior of UrCy-PPG in more detail using differential scanning calorimetry (DSC). Fig. 1a presents the DSC traces for AcCy-PPG, Cy-PPG and UrCy-PPG. UrCy-PPG exhibited a clear glass transition temperature (T_g) of −48.2 °C, a broad melting temperature of 100.3 °C and a heat of fusion (ΔH) of 7.8 J g^{-1}, whereas AcCy-PPG and Cy-PPG only displayed T_g values at −34.5 and −19.5 °C, respectively. This implies that attachment of UrCy moieties to the PPG ends promoted closer packing of the polymer chains and exhibited phase separation between the UrCy and PPG chains, resulting in the formation of a semi-crystalline polymer with significantly altered macroscopic properties.

To further verify the DSC data, *in situ* synchrotron wide-angle X-ray scattering (WAXS) measurements were performed at 25 °C to analyze the microstructural evolution of these supramolecular polymers. As shown in Fig. 1b, the WAXS profiles revealed the highly ordered lamellar microstructure of UrCy-PPG (q = 1 up to 5), with the first and most intense scattering peak at 1q of 0.92 nm^{-1}, corresponding to a *d*-spacing of 6.83 nm, reflecting the formation of self-complementary UrCy:UrCy interactions on the *d*-spacing of UrCy-PPG.[23,28] In contrast, AcCy-PPG and Cy-PPG showed typical amorphous patterns in WAXS, implying that the weak CMHB interactions between AcCy and Cy moieties tend to reduce the connectivity of the polymer chains, resulting in a single homogeneous amorphous phase within the polymer matrix. In other words, strong intermolecular dimerization of UrCy moieties leads to self-assembly of a closely packed crystalline/hard domain, thus inducing phase separation between the UrCy and PPG chains. These results also suggest that the hydrogen bonding strength of supramolecular polymers plays a dominant role in phase separation. In the higher q region of the WAXS patterns (Fig. 1b), UrCy-PPG exhibited two scattering peaks at q = 6.42 nm^{-1} (*d* = 0.98 nm) and 7.40 nm^{-1} (*d* = 0.85 nm), respectively. The peak at q = 6.42 nm^{-1} was attributed to the intermolecular distance of dimerized UrCy, *i.e.*, the length between these interaction domains.[29,30] The other peak at q = 7.40 nm^{-1} was attributed to the distance between the plane of closely-packed UrCy dimers, as a result of combining specific interactions with a regular crystal lattice structure.[31,32] Therefore, the multiple intense scattering peaks located at q = 7.40, 13.08 and 14.57 nm^{-1} correspond to the close stacking of UrCy moieties, as a consequence of crystallization due to self-assembly of UrCy end groups that tend to promote end-to-end alignment in an ordered microdomain. Compared to AcCy-PPG and Cy-PPG, the incorporation of UrCy moieties into PPG promoted efficient connection between neighboring polymer chains, resulting in the formation of a highly aligned lamellar microstructure with long-range order.

Since UrCy-PPG has an average molecular weight of approximately 1100 g mol^{-1} (Fig. S4†), the end-to-end distance of the PPG linker should be less than 4.0 nm. Based on the WAXS data in Fig. 1b, UrCy-PPG has a lamellar *d*-spacing of 6.83 nm, significantly higher than the theoretical polymer chain length, which is possibly attributed to complete chain alignment and extension of the flexible PPG backbone during the self-assembly process. To explore the mechanism responsible for the larger *d*-spacing within the PU-UrCy system, we performed variable-temperature WAXS and small-angle X-ray scattering (SAXS) experiments to directly observe the self-assembly process of UrCy-PPG. As shown in Fig. 2, results similar to the room temperature WAXS results discussed above were obtained, in which UrCy-PPG exhibited a long-range ordered lamellar structure at 30 °C. Surprisingly, as the temperature was gradually increased from 30 to 100 °C, a new 1q′ peak at 1.57 nm^{-1} (*d* = 4.00 nm) appeared with the gradual disappearance of the 1q peak at 0.92 nm^{-1} (*d* = 6.83 nm), suggestive of a change in the domain spacing of the lamellar morphology. Due to the presence of flexible propylene oxide linkages in the polymer backbone, the lamellar structure and transition mechanisms of UrCy-PPG can be reasonably explained by a theory of chain contraction/extension transition in linear polymers. At temperatures below 80 °C, flexible PPG chains adopt closely packed structures, resulting in both extension of the polymer backbone and an increase in lamellar *d*-spacing due to the supramolecular interactions contributed by the intermolecular quadruple hydrogen bonding interactions between UrCy moieties (Scheme 1). Upon further heating to between 80 and 100 °C, the intermolecularly hydrogen-bonded form of UrCy may alter its conformation to enhance the thermodynamic stability of the supramolecular structure, thus leading to a transition from an extended lamellar microstructure to a contractile lamellar microstructure, with a corresponding decrease in lamellar *d*-spacing from 6.83 nm to 4.00 nm. Therefore, we hypothesize that temperature-induced extension/contraction of the polymer chains is related to the hydrogen-bonded transition structures within UrCy-PPG. However, as the temperature was further

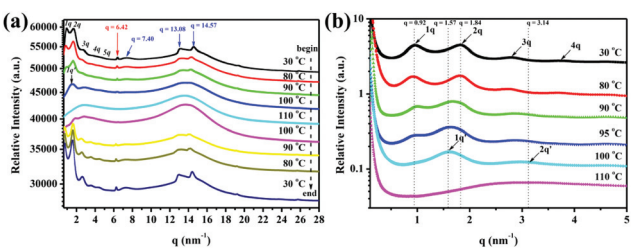

Fig. 2 Variable-temperature (a) WAXS and (b) SAXS data for UrCy-PPG recorded during heating and cooling.

This journal is © The Royal Society of Chemistry 2017

Published on 26 April 2017. Downloaded by Synchrotron Radiation Library on 12/12/2017 06:20:03.

increased from 100 to 110 °C, the periodic lamellar pattern converted into an amorphous phase, indicating that the long-range ordered structure fully disappeared due to complete dissociation of the hydrogen-bonded UrCy dimers and melting of the lamellar structure. Conversely, this scattering pattern spontaneously returned to the original lamellar structure arrangement when the sample was cooled slowly to 30 °C (Fig. 2a). This result strongly indicates that UrCy end-functionalized hydrogen-bonded supramolecular complexes can undergo stable thermoreversible transitions between ordered crystalline and disordered amorphous structures. As homogeneous melting is an important process of phase transition, microphase separation occurs due to the repulsive interaction between the soft and hard segments of UrCy-PPG when hierarchical self-assembly of the hydrogen-bond crystalline domains into the lamellar phases occurs, creating the arrangement of a flexible PPG segment.[33,34]

To gain further insight into the dynamic behavior of temperature-induced microstructural transformation, we subjected UrCy-PPG to variable-temperature Fourier transform infrared (VT-FTIR) measurements. Fig. 3a shows the VT-FTIR spectra of the N–H stretching region of UrCy-PPG at 30 °C. The characteristic peaks at frequencies of 3178 and 3216 cm^{-1} correspond to the stretching vibration of strongly hydrogen-bonded N–H groups,[35] indicating that the UrCy moieties within the polymer matrix provide highly directional and non-self-complementary interactions. Upon heating from 30 to 110 °C, the strong hydrogen-bonded N–H peaks at 3178 and 3216 cm^{-1} shifted to slightly higher wavenumbers and the UrCy N–H stretching vibration at 3239 cm^{-1} gradually appeared. This finding indicates that heating did not significantly affect the hydrogen-bonded dimeric interactions between UrCy groups and that UrCy-PPG forms a stable thermoreversible polymer containing CMHB complexes in the bulk state. In the 1600 to 1780 cm^{-1} wavenumber range of the VT-FTIR spectrum (Fig. 3b), several carbonyl stretch peaks for UrCy-PPG were observed at 30 °C; four peaks at 1619, 1658, 1705 and 1729 cm^{-1} corresponding to hydrogen-bonded urea, strongly-associated UrCy, and amorphous and crystalline ester-carbonyl groups, respectively. As the temperature was increased from 30 to 100 °C, three new peaks at 1625, 1680 and 1719 cm^{-1} gradually appeared, along with the disappearance of the peaks at 1619 and 1705 cm^{-1}, suggestive of an alteration to the hydrogen-bonded complexes of the cytosine ring. Interestingly, the characteristic peak of the hydrogen-bonded cytosine carbonyl group at 1658 cm^{-1} shifted slightly toward a lower wavenumber (at 1652 cm^{-1}). This observation strongly implies that the strong hydrogen bonding ability of the cytosine moiety remains virtually unaffected during the heating process, and the melting behavior of UrCy-PPG is not associated with disruption of the cytosine–urea hydrogen bond interactions. However, when the temperature was further increased above 100 °C, the amorphous ester-carbonyl peak at 1719 cm^{-1} clearly appeared as the strongly crystalline and hydrogen-bonded carbonyl peaks at 1705 and 1619 cm^{-1} almost completely disappeared, thereby forming new characteristic peaks at 1625, 1652 and 1680 cm^{-1}. These results show good agreement with the variable-temperature WAXS/SAXS experimental data (Fig. 2), further confirming that the hydrogen bond structures of the UrCy groups become dissociated and rearranged as the temperature increases. In order to confirm the phase transition mechanism of UrCy-PPG, we performed variable-temperature nuclear magnetic resonance (VT-NMR) experiments in tetrachloroethane-d_2 solution. As shown in Fig. S5,† the proton VT-NMR spectra illustrate the UrCy proton signals for UrCy-PPG at 25 °C, in which the characteristic protons were observed at 10.80 (H_1), 8.77 (H_2), 7.80 (H_3) and 7.61 (H_4) ppm, corresponding to the formation of the quadruple hydrogen bonded complex between UrCy moieties.[21,23] Upon heating from 25 to 105 °C, the protons at H_2 and H_3 did not show any significant changes; however, the protons at H_1 and H_4 shifted substantially upfield to 9.72 and 7.13 ppm, respectively, suggestive of a change in the nature of hydrogen bonded complexes between urea and cytosine groups (Fig. 3c). Based on these findings, we reasonably conjecture that these effects are a consequence of the two-state equilibrium between unfolded and folded structures. As illustrated in Fig. 3c, increasing the temperature induced a hydrogen-bonded structural transition from an intermolecularly-favorable quadruple hydrogen-bonded DDAA-dimer (at below 90 °C) to an intramolecularly-favorable dual hydrogen-bonded DA-dimer (at above 90 °C). In other words, the smaller lamellar *d*-spacing observed at high temperatures can be attributed to the structural folding-induced formation of intramolecular dual hydrogen-bonded

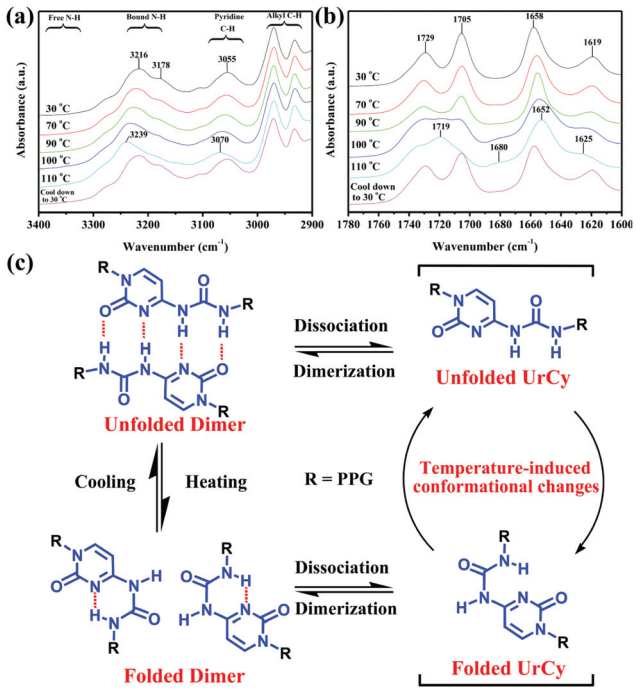

Fig. 3 Variable-temperature FTIR spectra for the UrCy-PPG in the ranges from (a) 2900–3400 and (b) 1600–1780 cm^{-1}. (c) Structural representation of temperature-induced switching between unfolded and folded UrCy dimers.

Published on 26 April 2017. Downloaded by Synchrotron Radiation Library on 12/12/2017 06:20:03.

arrays (Fig. 2b and 3c). In contrast, the larger lamellar *d*-spacing at low temperatures is presumably the result of the perfect ordering of the quadruple hydrogen-bonded array leading to close packing of the polymer chains and a high degree of microphase separation, resulting in the formation of long-range ordered supramolecular polymers with larger *d*-spacing between layers.

As the microstructural stability of supramolecular polymers is mainly dependent on the viscoelastic nature of the polymer matrix, we further investigated the dynamic viscoelastic properties of UrCy-PPG *via* rheological measurements at different shear strains (γ). All rheological measurements were carried out between 75 and 120 °C. The natural logarithm of dynamic storage modulus (G'), loss modulus (G'') and complex viscosity were plotted against temperature, as shown in Fig. S6.† The γ applied was lower than 10%, and the rheological response of UrCy-PPG at 95 °C exhibited a sharp phase transition from highly elastic-like ($G' > G''$) behavior to predominantly viscous-like ($G'' > G'$) behavior (Fig. S6a and S6b†). At the same time, the viscosity of UrCy-PPG decreased significantly from 1.0×10^5 Pa s at 90 °C to 5.1 Pa s at 102 °C. This phenomenon indicates that the supramolecular interactions between individual UrCy moieties are temperature-dependent, with an interesting order–disorder transition from a crystalline solid to the liquid state when the temperature increases, even though the structural conformation of UrCy dimers can rearrange readily to form a specific hydrogen-bonded array. When the γ applied was increased to 20%, the phase transition temperature significantly decreased to 85 °C, implying that the hydrogen-bonded structural transition is initiated under low shear conditions (Fig. S6c†). However, when the γ applied exceeded a critical value (27.4%; Fig. S6d–f†), UrCy-PPG changed to a viscous-like state and lost its characteristic reversible phase transition feature, leading to a substantial reduction in viscosity. It has been suggested that the growth of the supramolecular polymer is inhibited in the presence of high γ, possibly due to the promotion of a structural transition from an intermolecular quadruple hydrogen-bonded array (at low γ) to an intramolecular dual hydrogen-bonded array (at high at low γ), as illustrated in Scheme S2.† This intriguing behavior leads us to investigate the shear-induced microstructural transitions in more detail. Samples were prepared using a cone and plate-type rheometer at 80 °C and different γ for 10 min, and SAXS measurements were conducted at 25 °C. The SAXS patterns of UrCy-PPG under different γ are shown in Fig. 4a–d. In the initial state (γ = 5%), UrCy-PPG exhibited characteristic long-range ordered lamellar structures (q = 1 to 3), indicating that 5% shear did not significantly affect the lamellar structures of UrCy-PPG. When γ was increased eight-fold from 5% to 40%, the 2q peak at 1.86 nm^{-1} shifted to a remarkably lower q value and the intensity of the 1q peak at 0.93 nm^{-1} slightly reduced. Surprisingly, as γ was further increased above 80%, the first 1q peak of UrCy-PPG corresponding to a *d*-spacing of 6.8 nm disappeared, implying that the long-range order lamellar structure was completely destroyed under high shear conditions. In addition, UrCy-PPG exhibited a new long-period peak (1q′) at

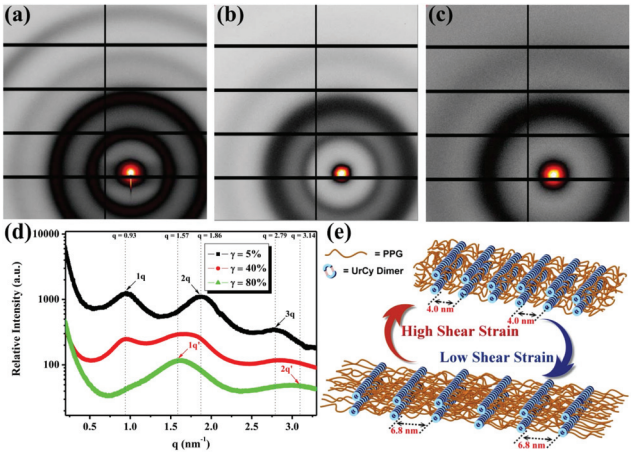

Fig. 4 (a–c) Two-dimensional and (d) one-dimensional SAXS patterns for UrCy-PPG at shear stresses (γ) of (a) 5%, (b) 40% and (c) 80%. (e) Suggested processes of shear-induced transitions between the extended and contracted lamellar microstructures in the UrCy-PPG system.

1.57 nm^{-1}, corresponding to a *d*-spacing of 4.00 nm, indicating short *d*-spacing intermolecular connections between the nearest-neighbor UrCy moieties. This observation is in close agreement with the variable temperature WAXS/SAXS results (Fig. 2). Therefore, we conclude that the change in the *d*-spacing of the lamellar structure is dominated by chain–chain movement and relaxation of closely packed structures within the flexible polymer segment. In other words, shear-induced transitions between extended and contracted lamellar microstructures may be attributed to the hydrogen-bonded transition structures within UrCy-PPG (Fig. 4e and Scheme S2†). Collectively, these observations indicate that this newly-devised macromer represents a highly efficient dynamic material that can rapidly change its viscoelastic behavior to a phase transition behavior, and also undergoes microstructural rearrangement under various shear and temperature conditions with good dynamic reversibility and structural stability.

Conclusions

In conclusion, we have successfully developed a feasible, simple strategy for preparing a low-molecular-weight supramolecular polymer, UrCy-PPG, based on the presence of self-complementary quadruple hydrogen-bonded UrCy moieties and oligomeric PPG. In contrast to conventional intensively studied oligomers, incorporating UrCy motifs into the end of PPG chains provides a route for spontaneous self-assembly towards the formation of long-range-ordered lamellar structures in the solid state that exhibit a number of attractive properties, including excellent thermoreversible and viscoelastic behavior, as well as rapid and stable hydrogen-bonded structural transitions. Due to the ease of altering the hydrogen bond structures of the UrCy moieties from quadruple to dual hydrogen-bonded arrays by tuning the environmental tempera-

 This journal is © The Royal Society of Chemistry 2017

Published on 26 April 2017. Downloaded by Synchrotron Radiation Library on 12/12/2017 06:20:03.

ture, UrCy-PPG can be easily tailored to obtain the desired lamellar structure with different interlayer spacings, a feature that is extremely rare yet highly desirable among supramolecular polymers and low-molecular-weight oligomers. More excitingly, small angle X-ray scattering clearly demonstrated shear-induced microstructural transitions in the UrCy-PPG system, which confers a dynamic self-organizing capability to manipulate the transition between the extended and contracted lamellar microstructures. Therefore, this newly-developed material is not only able to control its self-assembly and self-organization during the creation of ordered systems, but can also dynamically manipulate the periodic spacing of the lamellar morphology under elevated temperature and shear conditions, making this material highly attractive for the development of high-performance polymer-based supramolecular materials. Overall, the present study provides a new, effective strategy to enable controlled self-sorting organization of multifunctional supramolecular polymers that could be applied to tune the microstructural features and self-assembly ability of functional polymers.

Acknowledgements

We thank the National Synchrotron Radiation Research Center (NSRRC, Taiwan) for the support in the SAXS/WAXS measurements. This study was supported financially by the Ministry of Science and Technology, Taiwan (contract no. MOST 104-2221-E-011-153 and MOST 105-2628-E-011-006-MY2).

References

1 T. F. A. de Greef and E. W. Meijer, *Nature*, 2008, **453**, 171–173.
2 A. Harada, Y. Takashima and H. Yamaguchi, *Chem. Soc. Rev.*, 2009, **38**, 875–882.
3 M. Burnworth, L. Tang, J. R. Kumpfer, A. J. Duncan, F. L. Beyer, G. L. Fiore, S. J. Rowan and C. Weder, *Nature*, 2011, **472**, 334–337.
4 T. Aida, E. W. Meijer and S. I. Stupp, *Science*, 2012, **335**, 813–817.
5 L. Yang, X. Tan, Z. Wang and X. Zhang, *Chem. Rev.*, 2015, **115**, 7196–7239.
6 S. Sivakova and S. J. Rowan, *Chem. Soc. Rev.*, 2005, **34**, 9–21.
7 H. J. Schneider, *Angew. Chem., Int. Ed.*, 2009, **48**, 3924–3977.
8 S. Seittert and J. Sprakel, *Chem. Soc. Rev.*, 2012, **41**, 909–930.
9 (*a*) B. Zheng, F. Wang, S. Dong and F. Huang, *Chem. Soc. Rev.*, 2012, **41**, 1621–1636; (*b*) Z. Zhang, Y. Luo, J. Chen, S. Dong, Y. Yu, Z. Ma and F. Huang, *Angew. Chem., Int. Ed.*, 2011, **50**, 1397–1401; (*c*) S. Dong, Y. Luo, X. Yan, B. Zheng, X. Ding, Y. Yu, Z. Ma, Q. Zhao and F. Huang, *Angew. Chem., Int. Ed.*, 2011, **50**, 1905–1909; (*d*) X. Yan, D. Xu, X. Chi, J. Chen, S. Dong, X. Ding, Y. Yu and F. Huang, *Adv. Mater.*, 2012, **24**, 362–369; (*e*) X. Ji, Y. Yao, J. Li, X. Yan and F. Huang, *J. Am. Chem. Soc.*, 2013, **135**, 74–77.
10 M. A. C. Stuart, *Nat. Mater.*, 2010, **9**, 101–113.
11 S. Y. Dong, B. Zheng, F. Wang and F. H. Huang, *Acc. Chem. Res.*, 2014, **47**, 1982–1994.
12 J. L. Sessler, C. M. Lawrence and J. Jayawickramarajah, *Chem. Soc. Rev.*, 2007, **36**, 314–325.
13 S. L. Li, T. Xiao, C. Lin and L. Wang, *Chem. Soc. Rev.*, 2012, **41**, 5950–5968.
14 L. Brunsveld, B. J. B. Folmer, E. W. Meijer and R. P. Sijbesma, *Chem. Rev.*, 2001, **101**, 4071–4098.
15 J. L. Sessler and J. Jayawickramarajah, *Chem. Commun.*, 2005, 1939–1949.
16 F. H. Beijer, R. P. Sijbesma, H. Kooijman, A. L. Spek and E. W. Meijer, *J. Am. Chem. Soc.*, 1998, **120**, 6761–6769.
17 E. Kolomiets and J.-M. Lehn, *Chem. Commun.*, 2005, 1519–1521.
18 W. H. Binder, S. Bernstorff, C. Kluger, L. Petraru and M. J. Kunz, *Adv. Mater.*, 2005, **17**, 2824–2828.
19 R. Schmidt, M. Stolte, M. Grüne and F. Würthner, *Macromolecules*, 2011, **44**, 3766–3776.
20 M. Guo, L. M. Pitet, H. M. Wyss, M. Vos, P. Y. W. Dankers and E. W. Meijer, *J. Am. Chem. Soc.*, 2014, **136**, 6969–6977.
21 V. G. H. Lafitte, A. E. Aliev, P. N. Horton, M. B. Hursthouse, K. Bala, P. Golding and H. C. Hailes, *J. Am. Chem. Soc.*, 2006, **128**, 6544–6545.
22 E. Greco, A. E. Aliev, V. G. H. Lafitte, K. Bala, D. Duncan, L. Pilon, P. Golding and H. C. Hailes, *New J. Chem.*, 2010, **34**, 2634–2642.
23 C. C. Cheng, F. C. Chang, J. H. Wang, Y. L. Chu, Y. S. Wang, D. J. Lee, W. T. Chuang and Z. Xin, *RSC Adv.*, 2015, **5**, 76451–76457.
24 C. C. Cheng, F. C. Chang, J. H. Wang, J. K. Chen, Y. C. Yen and D. J. Lee, *Nanoscale*, 2016, **8**, 723–728.
25 C. C. Cheng and D. J. Lee, *RSC Adv.*, 2016, **6**, 38223–38227.
26 (*a*) C. C. Cheng, Z.-S. Liao, J. J. Huang, D. J. Lee and J. K. Chen, *Dyes Pigm.*, 2017, **137**, 284–292; (*b*) C. C. Cheng, J. J. Huang, A. A. Muhable, Z. S. Liao, S. Y. Huang, S. C. Lee, C. W. Chiu and D. J. Lee, *Polym. Chem.*, 2017, **8**, 2292–2298.
27 C. C. Cheng, M. C. Liang, Z.-S. Liao, J. J. Huang and D. J. Lee, *Macromol. Biosci.*, 2017, DOI: 10.1002/mabi.201600370.
28 C. C. Cheng, I. H. Lin, Y. C. Yen, C. W. Chu, F. H. Ko, X. Wang and F. C. Chang, *RSC Adv.*, 2012, **2**, 9952–9957.
29 T. Shimizu, R. Iwaura, M. Masuda, T. Hanada and K. Yase, *J. Am. Chem. Soc.*, 2001, **123**, 5947–5955.
30 J. Miao and L. Zhu, *Chem. Mater.*, 2010, **22**, 197–206.
31 C. A. Hunter, K. R. Lawson, J. Perkins and C. J. Urch, *J. Chem. Soc., Perkin Trans. 2*, 2001, 651–669.
32 R. Ziessel, G. Pickaert, F. Camerel, B. Donnio, D. Guillon, M. Cesario and T. Prange, *J. Am. Chem. Soc.*, 2004, **126**, 12403–12413.
33 J. Cortese, C. Soulié-Ziakovic, M. Cloitre, S. Tencé-Girault and L. Leibler, *J. Am. Chem. Soc.*, 2011, **133**, 19672–19675.
34 J. Cortese, C. Soulié-Ziakovic, S. Tencé-Girault and L. Leibler, *J. Am. Chem. Soc.*, 2012, **134**, 3671–3674.
35 O. Uzun, A. Sanyal, H. Nakade, R. J. Thibault and V. M. Rotello, *J. Am. Chem. Soc.*, 2004, **126**, 14773–14777.